Geophysical Research Letters

RESEARCH LETTER
10.1029/2021GL095883

Hydroclimate and ENSO Variability Recorded by Oxygen Isotopes From Tree Rings in the South American Altiplano

Milagros Rodriguez-Caton[1,2], Laia Andreu-Hayles[1,3,4], Valérie Daux[5], Mathias Vuille[6], Arianna M. Varuolo-Clarke[1], Rose Oelkers[1], Duncan A. Christie[7,8], Rosanne D'Arrigo[1], Mariano S. Morales[9,10], Mukund Palat Rao[1,11,12], Ana M. Srur[9], Françoise Vimeux[13,14], and Ricardo Villalba[9]

[1]Tree Ring Laboratory, Lamont-Doherty Earth Observatory of Columbia University, Palisades, NY, USA, [2]Department of Plant Sciences, University of California, Davis, CA, USA, [3]CREAF, Bellaterra (Cerdanyola del Vallés), Barcelona, Spain, [4]ICREA, Barcelona, Spain, [5]Laboratoire des Sciences du Climat et de l'Environnement, CEA/CNRS/UVSQ/IPSL, Gif-sur-Yvette, France, [6]Department of Atmospheric and Environmental Sciences, State University of New York at Albany, Albany, NY, USA, [7]Laboratorio de Dendrocronología y Cambio Global, Instituto de Conservación Biodiversidad y Territorio, Universidad Austral de Chile, Valdivia, Chile, [8]Center for Climate and Resilience Research, (CR)2, Santiago, Chile, [9]Instituto Argentino de Nivología, Glaciología y Cs. Ambientales (IANIGLA), CONICET Mendoza, Argentina, [10]Laboratorio de Dendrocronología, Universidad Continental. Huancayo, Peru, [11]Cooperative Programs for the Advancement of Earth System Science, University Corporation for Atmospheric Research, Boulder, CO, USA, [12]Department of Plant Science, University of California, Davis, CA, USA, [13]HydroSciences Montpellier (HSM), UMR 5151 (UM, CNRS, IRD), Montpellier, France, [14]Institut Pierre Simon Laplace (IPSL), Laboratoire des Sciences du Climat et de l'Environnement (LSCE), UMR 8212 (CEA, CNRS, UVSQ), Gif-sur-Yvette, France

Key Points:

- Tree-ring stable oxygen isotopes of *Polylepis tarapacana* record austral summer precipitation variability in the South American Altiplano
- El Niño-Southern Oscillation is imprinted in the tree-ring oxygen isotopes with a stronger signal toward the north of the studied area

Supporting Information:

Supporting Information may be found in the online version of this article.

Correspondence to:

M. Rodriguez-Caton,
milagros@ldeo.columbia.edu;
milagrosrodriguezc@gmail.com

Citation:

Rodriguez-Caton, M., Andreu-Hayles, L., Daux, V., Vuille, M., Varuolo-Clarke, A. M., Oelkers, R., et al. (2022). Hydroclimate and ENSO variability recorded by oxygen isotopes from tree rings in the South American Altiplano. *Geophysical Research Letters*, *49*, e2021GL095883. https://doi.org/10.1029/2021GL095883

Received 10 SEP 2021
Accepted 3 JAN 2022

Abstract Hydroclimate variability in tropical South America is strongly regulated by the South American Summer Monsoon (SASM). However, past precipitation changes are poorly constrained due to limited observations and high-resolution paleoproxies. We found that summer precipitation and the El Niño-Southern Oscillation (ENSO) variability are well registered in tree-ring stable oxygen isotopes ($\delta^{18}O_{TR}$) of *Polylepis tarapacana* in the Chilean and Bolivian Altiplano in the Central Andes (18–22°S, ~4,500 m a.s.l.) with the northern forests having the strongest climate signal. More enriched $\delta^{18}O_{TR}$ values were found at the southern sites likely due to the increasing aridity toward the southwest of the Altiplano. The climate signal of *P. tarapacana* $\delta^{18}O_{TR}$ is the combined result of moisture transported from the Amazon Basin, modulated by the SASM, ENSO, and local evaporation, and emerges as a novel tree-ring climate proxy for the southern tropical Andes.

Plain Language Summary Understanding past climatic changes in the Central Andes in tropical South America is of great importance to contextualize current hydroclimatic conditions. Here, we present the first *P. tarapacana* tree-ring stable oxygen isotope ($\delta^{18}O_{TR}$) chronologies and analyze their value as environmental records for this region. Locally known as queñoa, *P. tarapacana* grows in the South American Altiplano from 16°S to 23°S at very high elevations (up to 5,100 m a.s.l), making it the highest elevation tree species worldwide. We analyze *P. tarapacana* $\delta^{18}O_{TR}$ from 1950 to present and find that it registers precipitation changes in the Altiplano and the El Niño - Southern Oscillation (ENSO). We suggest that $\delta^{18}O_{TR}$ is likely affected by soil evaporation and leaf transpiration due to the high solar radiation and aridity in the Altiplano, leading to an enrichment in $\delta^{18}O_{TR}$ values with a more pronounced effect at the more arid sites. *P. tarapacana* $\delta^{18}O_{TR}$ reflects the atmospheric processes transporting moisture to the Altiplano and the influence of local evaporation. Our findings are relevant for generating robust hydroclimate reconstructions in the Central Andes to improve circulation models and provide better management of water resources in tropical South America.

1. Introduction

Droughts in the South American Altiplano, a semiarid high-elevation plateau located in the Central Andes, affect millions of people and produce large economic losses across the Andes and the adjacent arid lowlands (Cane-do-Rosso et al., 2021). Some studies (Minvielle & Garreaud, 2011; Neukom et al., 2015) have projected a future increase in drought over the Altiplano, although the assumptions on which these projections were based have recently been questioned (Segura et al., 2020). Thus, understanding hydroclimatic changes in the Altiplano is of great importance to assess the vulnerability of natural habitats and human activities to water scarcity.

The South American Summer Monsoon (SASM) system dominates most of the South American seasonal hydroclimate (Marengo et al., 2012; Vuille et al., 2012). The buildup of the Bolivian High, an anticyclonic system situated over Bolivia, during the austral summer is a key atmospheric feature associated with the SASM. The Bolivian High blocks the atmospheric circulation from the west, allowing the mid-to upper-level easterly winds to entrain near-surface upslope flow and moisture transport from the Amazon basin toward the Altiplano (Garreaud et al., 2003). This moisture originates in the Atlantic Ocean and is transported toward the Amazon Basin by easterly trade winds during the austral summer (Lenters & Cook, 1997). Moisture is recycled over the Amazon basin before being transported toward the Altiplano (Garreaud, 1999; Segura et al., 2020). Thus, most precipitation (i.e., 75%–90%) in the Altiplano falls during the austral summer (December to March; Garreaud et al., 2003; Vuille & Keimig, 2004), coincident with the mature phase of SASM from December to February (Raia & Cavalcanti, 2008), although occasional winter snowfall sourced from the Pacific is possible (Vuille & Ammann, 1997). At interannual scales, this moisture transport to the Altiplano from the Amazon Basin is greatly influenced by sea surface temperatures (SST) in the tropical Pacific (Sulca et al., 2018) with below (above) normal precipitation during El Niño (La Niña) years (Vuille, 1999).

There are few instrumental records of climate in tropical South America prior to 1950, especially in the high Andes including the Altiplano. This is further compounded by the high interannual and spatial precipitation variability in the region due to its complex topography and the multitude of climate drivers (Vuille & Keimig, 2004). Long-term high-resolution climate proxies are therefore of great importance to extend climate information into the past and to evaluate the present climate dynamics in multicentennial time scales. Tree rings are high-resolution (annual to subannual) climate proxies with proven value for climate reconstructions. For more than a decade, a great effort has been made to expand the South American tree-ring network to the tropical Andes with special emphasis on the semiarid western Altiplano where *Polylepis tarapacana* grows (16°–23°S; Argollo et al., 2004; Christie et al., 2009; Morales et al., 2004, 2012, 2020; Moya & Lara, 2011; Soliz et al., 2009). This species forms the world's highest elevation forests (4,000–5,100 m a.s.l.; Braun, 1997). Given the quality of its ring-width climate signal and its longevity of up to 750 years, it represents the most valuable paleoclimate archive to develop tree ring-based reconstructions in the tropical Andes. However, very little research has been done to evaluate the climate signal in the stable oxygen isotopes contained in tree-ring cellulose of *P. tarapacana* (Ballantyne et al., 2011; Rodriguez-Caton et al., 2021).

Previous studies have shown that the degree of moisture recycling and rainout upstream over the Amazon Basin largely controls $\delta^{18}O$ in precipitation over the tropical and Central Andes and the Bolivian lowlands (Baker et al., 2015; Hoffmann et al., 2003; Kanner et al., 2013; Vimeux et al., 2005, 2011; Vuille & Werner, 2005; Vuille et al., 2012). These studies were based on models and natural archives mostly located north of 19°S; thus, less is known about the driest and most distal part of the SASM domain located at the southwestern margin of the Altiplano adjacent to the Atacama Desert (Galewsky & Samuels-Crow, 2015).

The development of a network of *P. tarapacana* oxygen isotope chronologies emerges as a valuable tool to complement the present collection of stable oxygen isotope records from the tropical Andes (Vuille et al., 2012), mainly from ice cores, lake sediments, and speleothems, to infer the local- and large-scale climate variability and changes in the region during the last millennium. Stable oxygen isotopes in tree rings ($\delta^{18}O_{TR}$) reflect the $\delta^{18}O$ signal of the water absorbed by the roots but also other processes, such as soil evaporation and leaf transpiration. While water absorption by roots is a non-fractionating process (e.g., Bariac et al., 1990; Dawson & Ehleringer, 1993), soil evaporation and leaf transpiration (the process of plant water evaporation through leaf stomata) can result in enriched $\delta^{18}O_{TR}$ signatures due to preferential evaporation of the lighter isotope (^{16}O). Finally, during cellulose synthesis, oxygen atoms can be exchanged between phloem carbohydrates and xylem water, contributing to a higher imprint of source water (Cheesman & Cernusak, 2017; Gessler et al., 2009; Sternberg et al., 1986).

Here, we used four $\delta^{18}O_{TR}$ site chronologies of *P. tarapacana* spanning from 1950 to 2015 along a latitudinal-aridity gradient from 18°S to 22°S in the South American Altiplano to investigate the potential of this network to develop a precipitation reconstruction for the southern tropical Andes. Since, $\delta^{18}O_{TR}$ carries a strong signal of the water used by the trees, we hypothesize that our $\delta^{18}O_{TR}$ records reflect hydroclimate and thus register the SASM and ENSO variability in this region.

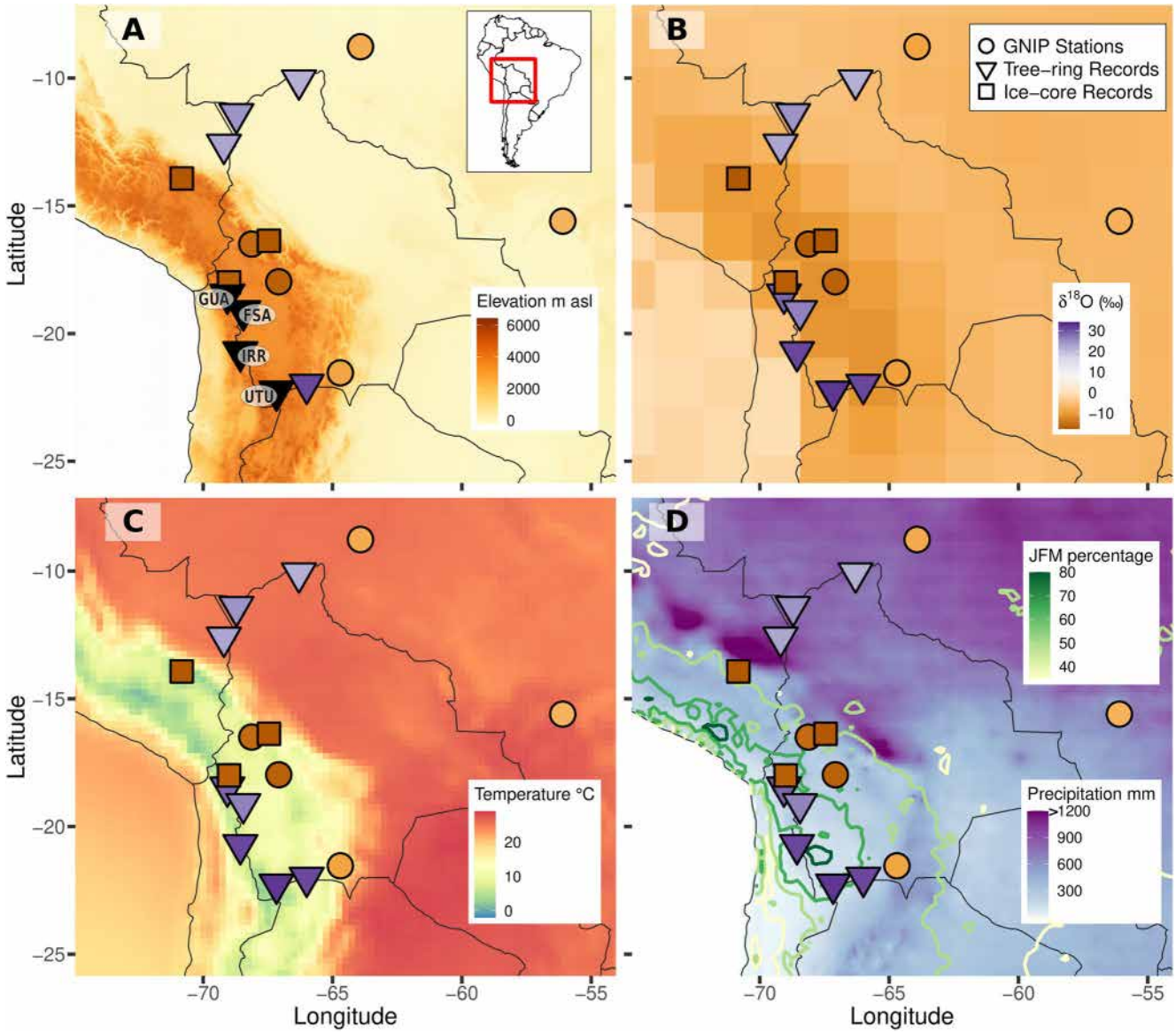

Figure 1. Topography, climate and $\delta^{18}O$ observations and proxy records in the Altiplano. (a) Elevation in meters above sea level (m a.s.l.). Black triangles with labels (GUA, FSA, IRR, and UTU) represent our four *Polylepis tarapacana* $\delta^{18}O_{TR}$ sites (Table S1 in Supporting Information S1) (b) IsoGSM mean precipitation $\delta^{18}O$ for austral summer (JFM) for 1979–2018 (c) ERA5 mean summer temperature (JFM) for 1979–2018 (d) CHIRPS mean total summer precipitation (JFM) for 1981–2020. Contours represent the percentage of annual precipitation falling during JFM (contour interval is 15, contours <35 are omitted). Location of $\delta^{18}O$ observations and proxy records (Table S2 in Supporting Information S1) is shown in all panels: mean JFM $\delta^{18}O$ (‰) in precipitation for GNIP stations (circles) for the periods depicted in Table S3 in Supporting Information S1, and annual $\delta^{18}O$ values for tree rings (triangles) and ice cores (squares) for the period 1950–1984. The symbols are colored according to the $\delta^{18}O$ ratio (‰), following the color bar in (b).

2. Data and Methods

2.1. Stable Oxygen Isotope Tree-Ring Records

Our annually resolved *P. tarapacana* $\delta^{18}O_{TR}$ site chronologies, Guallatire (GUA), Frente Sabaya (FSA), Irruputuncu (IRR), and Uturunco (UTU), span from 1950 to 2007–2015 and are located at ~4,500 m a.s.l. along a latitudinal-aridity gradient (Figure 1a, Table S1 in Supporting Information S1). Site characteristics and methods to develop the $\delta^{18}O_{TR}$ site chronologies can be found in Supporting Information S1 (Notes S1 and Table S1 in Supporting Information S1) and Rodriguez-Caton et al. (2021). High correlations between the four sites (Figure S1 in Supporting Information S1) supported merging the site $\delta^{18}O_{TR}$ chronologies and obtaining a composite *P. tarapacana* $\delta^{18}O_{TR}$ chronology by computing a robust mean of the four site chronologies. This

composite chronology is almost identical to the first principal component of the four chronologies (Figure S2b in Supporting Information S1), which explains around 79% of the total variance.

We analyzed other $\delta^{18}O$ paleoclimate proxy records based on the Altiplano and surrounding areas, as well as observed and reanalysis-based precipitation amounts and precipitation $\delta^{18}O$ (Figure 1, Table S2 in Supporting Information S1). The records include ice cores (Hoffmann et al., 2003; Thompson et al., 1984, 1998; Vimeux et al., 2009), $\delta^{18}O_{TR}$ from an individual *P. tarapacana* tree in Argentina (Ballantyne et al., 2011), and *Cedrela odorata* $\delta^{18}O_{TR}$ from tropical lowlands (Baker et al., 2015; Brienen et al., 2012). We calculated average $\delta^{18}O$ for 1954–1984, the common period between these proxies. Observed $\delta^{18}O$ in precipitation was obtained from the International Atomic Energy Agency-Global Network of Isotopes in Precipitation (IAEA-GNIP) from five stations closest to the study area (Figure 1, Table S3 in Supporting Information S1). We also used 2.5° grid resolution IsoGSM precipitation and precipitation $\delta^{18}O$ for the period 1979–2018 (Yoshimura et al., 2008). IsoGSM is an isotope-enabled reanalysis product that realistically portrays the $\delta^{18}O$ seasonal cycle and interannual variability in this region (Hurley et al., 2019).

2.2. Climate Data

We used Climatic Research Unit 0.5° grid resolution precipitation data set version 4.04 (CRU TS v.4.04; Harris et al., 2020) and CHIRPS precipitation data (Funk et al., 2015) based on remote sensing and meteorological stations for the period 1981–2020 with a spatial resolution of 0.05° × 0.05°. Monthly regional precipitation anomalies for 1950–2008 were also developed by averaging precipitation data from 32 meteorological stations located in the study region (Table S4 in Supporting Information S1; Rodriguez-Caton et al., 2021). We used 1° grid resolution ERA5 reanalysis temperature data (Dee et al., 2011) with a time span of 1979–2018 and global SST from NOAA NCDC Extended Reconstructed SST (ERSST version 3b) with a grid resolution of 2.0° × 2.0° from 1854 to present (Smith et al., 2008).

2.3. Relationships Between Climate and $\delta^{18}O$ Tree-Ring Records

We computed Pearson correlations between *P. tarapacana* $\delta^{18}O_{TR}$ chronologies and monthly precipitation anomalies for the common period 1950–2007 from August of the previous tree growing season to May of the current growing season using the R package *treeclim* (R Core Team, 2020; Zang & Biondi, 2015). The significance of the correlation coefficients was assessed by stationary bootstrapped confidence intervals (Biondi & Waikul, 2004).

Based on the results from monthly correlations, we used January, February, and March (JFM) precipitation for both CHIRPS (PP_{CHIRPS}) and CRU (PP_{CRU}) to develop spatial correlations with individual-site and composite *P. tarapacana* $\delta^{18}O_{TR}$ chronologies using Spearman rank. Field correlations were also computed between JFM precipitation (PP_{IsoGSM}) and precipitation $\delta^{18}O$ (PP $\delta^{18}O_{IsoGSM}$) from the isotope-enabled IsoGSM reanalysis data set, averaged over the location of our four study sites (three grid cells, since two locations shared a grid point).

To assess the influence of ENSO on $\delta^{18}O_{TR}$, we calculated spatial correlations between the $\delta^{18}O_{TR}$ chronologies and JFM global SST. Singular Spectral Analysis (Vautard, 1995; Vautard & Ghil, 1989) was performed to determine the dominant, nonstationary modes of variability of the frequency domains of the composite $\delta^{18}O_{TR}$ chronology and the JFM SSTs for the Niño 3.4 region (5°N–5°S, 170°W–120°W). We grouped the dominant modes of variability when they oscillated in similar frequencies (Notes S2 in Supporting Information S1). We also calculated probability density functions for $\delta^{18}O_{TR}$ and precipitation at each study site during El Niño/La Niña years and tested for significant differences according to the Mann-Whitney test (Figure S3 and Table S5 in Supporting Information S1).

3. Results

3.1. Precipitation $\delta^{18}O$ and Proxy Records in the Altiplano and Surrounding Areas

GNIP observations and ice-core proxy data show more negative $\delta^{18}O$ values as elevation increases (Figure 1a). This altitude effect likely reflects the first-order isotopic Rayleigh distillation with decreasing temperature (Figure 1c) and orographic precipitation as air masses approach the Andes and are lifted along the eastern slopes. This depletion in heavy isotopes as air masses move from the lowlands in the Amazon basin toward the higher

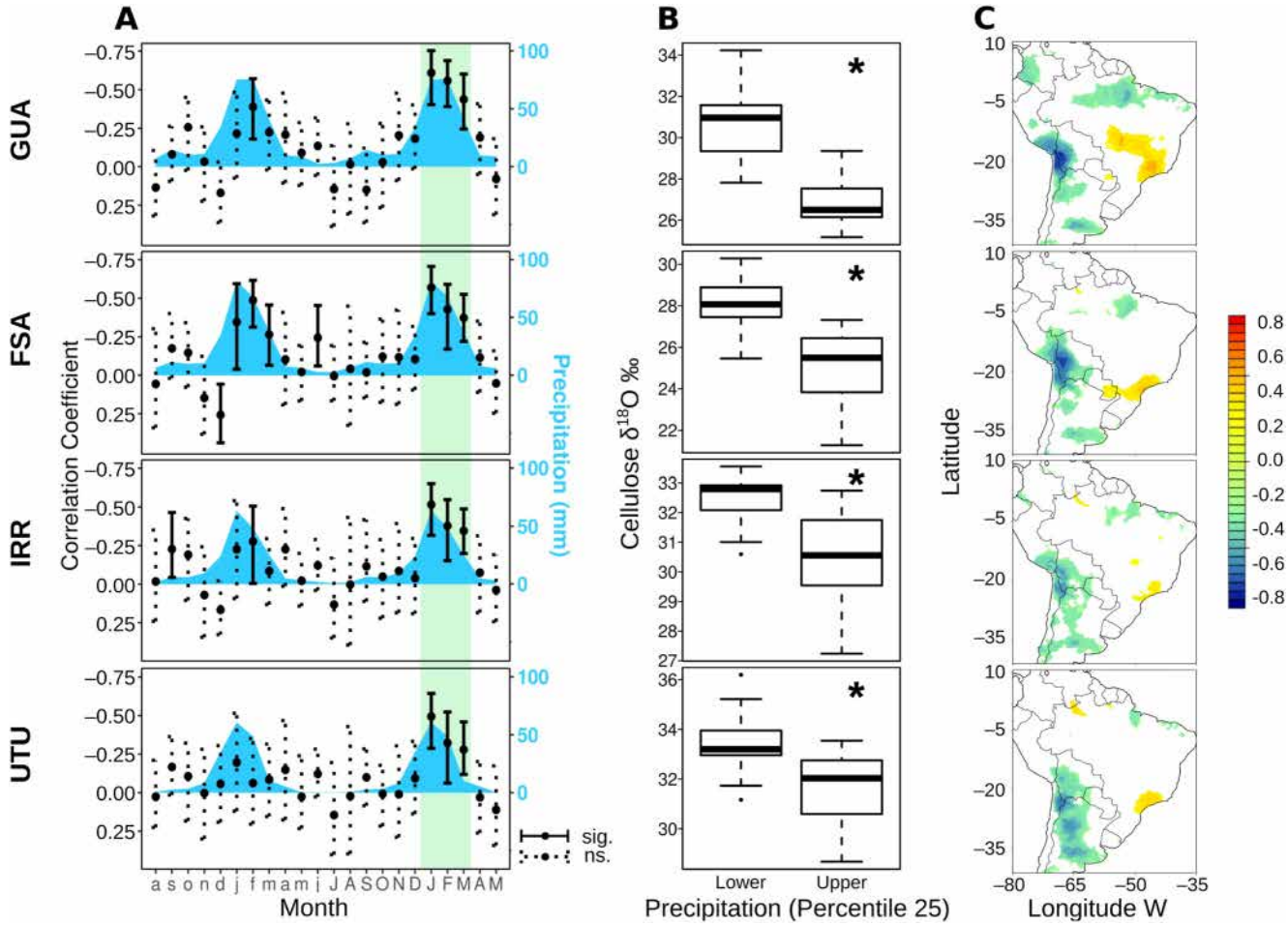

Figure 2. Relationships between *Polylepis tarapacana* $\delta^{18}O_{TR}$ chronologies and precipitation (a) Pearson correlation coefficients between $\delta^{18}O_{TR}$ and monthly regional precipitation based on meteorological stations (note that left *y* axis is inverted) for August of the previous growing season (lowercase) to May of the current growing season (uppercase) for 1950–2007. Vertical solid (dashed) lines represent significant (nonsignificant) bootstrap monthly correlation coefficients (alpha<0.05). Blue shading shows CHIRPS precipitation seasonality (1981–2020). Green vertical shading highlights current-year JFM (b) $\delta^{18}O_{TR}$ values during years of extreme (upper and lower percentiles [25%]) JFM precipitation. Asterisks indicate significant differences (Mann-Whitney, alpha <0.05) (c) Field Spearman correlations between the $\delta^{18}O_{TR}$ chronologies and JFM CRU precipitation; only significant values are shown (alpha <0.05).

altitude environments in the Altiplano is consistent with the distribution of precipitation $\delta^{18}O$ seen in IsoGSM (Figure 1b). However, *Polylepis* $\delta^{18}O_{TR}$ from the Altiplano has more positive $\delta^{18}O$ signatures than $\delta^{18}O_{TR}$ from *Cedrela* trees growing in lowland areas. This may be the result of increasing aridity and hence enhanced evaporation toward the southwest of the Andes (Figure 1d). Within our *P. tarapacana* network, an enrichment of $\delta^{18}O_{TR}$ is also evident toward the southern and more arid sites (Table S1 in Supporting Information S1).

3.2. Precipitation and ENSO Signal in *Polylepis tarapacana* $\delta^{18}O_{TR}$

At all sites, the most significant correlations between $\delta^{18}O_{TR}$ and monthly precipitation occur during the concurrent growing season (Figure 2a). The four *P. tarapacana* $\delta^{18}O_{TR}$ chronologies show a significant negative correlation with precipitation during the peak of the wet season (JFM), which coincides with the mature phase of SASM (Figures 1d and 2a). The highest correlations between $\delta^{18}O_{TR}$ and monthly precipitation occur in January, the rainiest month, with correlations about −0.6 (alpha <0.05) at the northernmost site GUA. Years with extremely low (high) precipitation are characterized by significantly more positive (negative) $\delta^{18}O_{TR}$ values (Figure 2b). The spatial extent of the CRU precipitation signal embedded in the $\delta^{18}O_{TR}$ records covers much of the Altiplano, reaching correlation coefficients close to −0.8 (alpha <0.05) at the northern sites of the study region (Figure 2c).

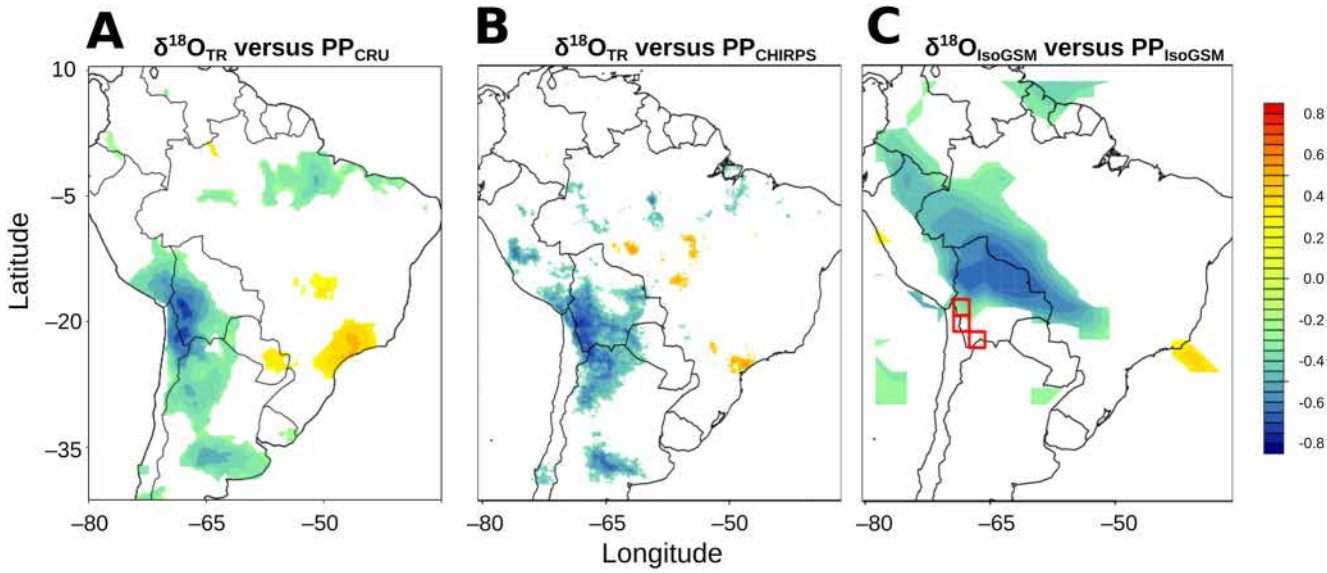

Figure 3. Spatial relationships between $\delta^{18}O$ and precipitation over South America. Spearman correlation coefficients between $\delta^{18}O_{TR}$ composite chronology and (a) gridded JFM CRU precipitation for the period 1950–2007 and (b) gridded JFM CHIRPS precipitation for the period 1981–2007 (c) Spearman correlation coefficients between PP $\delta^{18}O_{IsoGSM}$ averaged across the study sites (red boxes) and gridded JFM PP_{IsoGSM} for the period 1979–2007. Red boxes represent the three grids where our four sites are located and from where PP $\delta^{18}O_{IsoGSM}$ data were extracted. Only grid cells with significant correlation coefficients (alpha <0.05) are shown.

The significant negative correlation coeffcients between precipitation and the four $\delta^{18}O_{TR}$ site chronologies extend into the adjacent lowlands eastward from the Altiplano, indicating linkages to upstream rainout.

When moving from north to south along the aridity gradient in the Altiplano, the precipitation signal in $\delta^{18}O_{TR}$ weakens at both local (Figure 2a) and regional (Figure 2c) scales, but at the same time, the signal starts to propagate to the southeast toward the La Plata Basin (Figure 2c site UTU). However, overall, there is high consistency in the pattern of spatial correlation among the four study sites. This is further supported by 46%, 43%, and 42% of explained variance when using the composite $\delta^{18}O_{TR}$ chronology as a predictor for instrumental, CRU, and CHIRPS precipitation, respectively (Figure S4 in Supporting Information S1).

Across the southern tropical Andes, the composite *P. tarapacana* $\delta^{18}O_{TR}$ chronology shows a clear and consistent spatial correlation pattern with CRU and CHIRPS precipitation data (Figures 3a and 3b). These results are consistent with correlations between IsoGSM reanalysis precipitation (JFM PP_{IsoGSM}) and reanalysis precipitation $\delta^{18}O$ averaged across the four study sites (PP $\delta^{18}O_{IsoGSM}$; Figure 3c). However, while the sign of the correlation is the same, the location of the most significant correlation between PP_{IsoGSM} and PP $\delta^{18}O_{IsoGSM}$ is displaced upstream over the southwestern Amazon basin (Figure 3c).

The composite $\delta^{18}O_{TR}$ chronology shows strong correlations with SSTs over the Niño 3.4 region (Figure 4a), in particular at interannual (Figure 4b) and decadal (Figure 4c) scales as evidenced by shared spectral properties (Notes S2 in Supporting Information S1). These results demonstrate the ENSO signal imprinted on the $\delta^{18}O_{TR}$ of *P. tarapacana*.

Our results also show that precipitation amount is lower during El Niño than La Niña events along the aridity gradient with significant differences at the wetter sites GUA and FSA (Figure S3b and S5 in Supporting Information S1). Accordingly, the northernmost and wettest site GUA shows significantly more enriched $\delta^{18}O_{TR}$ during El Niño versus La Niña major events (Figure S3c in Supporting Information S1), as well as stronger correlations with central and eastern equatorial SSTs compared with the rest of the sites (Figure S3d in Supporting Information S1).

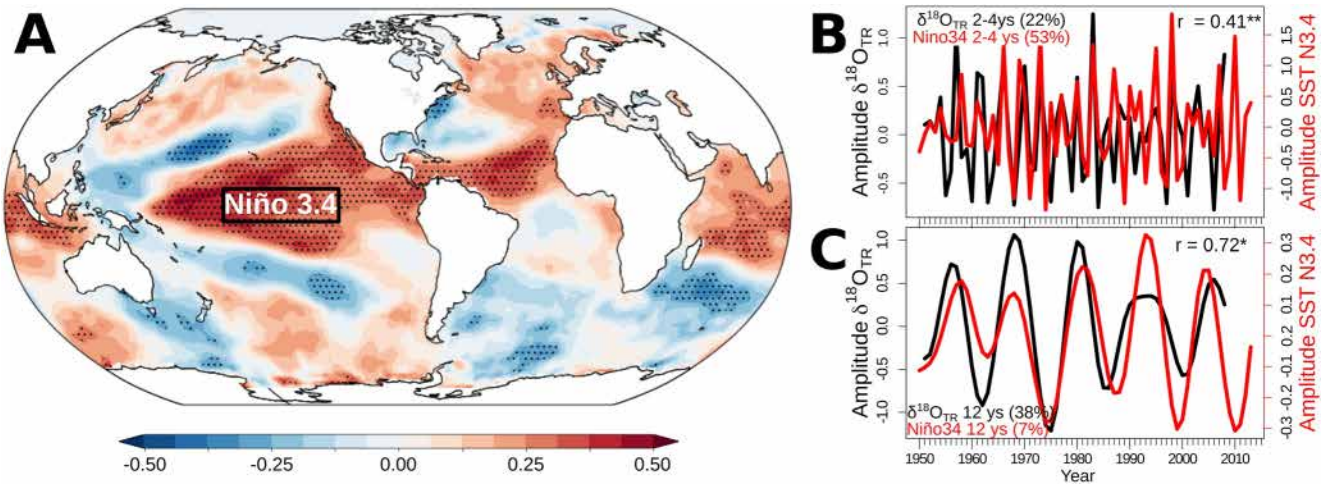

Figure 4. El Niño-Southern Oscillation signal in $\delta^{18}O_{TR}$ (a) Field Spearman correlations between the composite *Polylepis tarapacana* $\delta^{18}O_{TR}$ chronology and JFM SSTs for the period 1950–2007. Dotted areas indicate significant correlations (alpha<0.05). Time series of (b) interannual and (c) decadal frequency components of the $\delta^{18}O_{TR}$ and JFM SST. Variance explained by each frequency component is indicated between brackets, r indicates Pearson correlations coefficients between the components, and the stars indicate significance at alpha<0.1 (*) and alpha<0.05 (**) after accounting for the lower degrees of freedom due to the applied spectral filtering.

4. Discussion and Conclusions

Our findings reveal that *P. tarapacana* $\delta^{18}O_{TR}$ can serve as a valuable proxy for recording precipitation variability over the South American Altiplano. All the study sites show negative correlations between $\delta^{18}O_{TR}$ and precipitation (i.e., years with more rainfall correspond to more negative $\delta^{18}O_{TR}$) during austral summer (JFM) of the tree's current growing season. The sensitivity of our four $\delta^{18}O_{TR}$ records to summer precipitation agrees with the fact that most precipitation across this region falls during austral summer as a consequence of the SASM (Garreaud et al., 2003; Vuille et al., 2012). Indeed, the highest correlation occurs in January, which corresponds to the rainiest month in the study region. Although precipitation is also important during December, correlations were not significant for this month. This might be related to the fact that $\delta^{18}O_{TR}$ was measured from cellulose, which depending on the species and area can accumulate late in the growing season (Rathgeber et al., 2016).

The IsoGSM data indicate that precipitation $\delta^{18}O$ over the Altiplano is related to precipitation upstream over the Bolivian lowlands and southwestern Brazil (Figure 3c). This is consistent with previous studies, that show that precipitation $\delta^{18}O$ in the tropical Andes is dominated by Rayleigh-type fractionation during rainout over the Amazon basin (i.e., more negative precipitation $\delta^{18}O$ results from enhanced convective activity upstream, resulting in the depletion of the heavy isotopes in the remaining water vapor) (Risi et al., 2012; Vuille & Werner, 2005). The influence of upstream processes over the Amazon basin on the precipitation $\delta^{18}O$ has been observed in tree rings (Baker et al., 2016; Brienen et al., 2012), as well as in models and observations (Vimeux et al., 2005, 2011) in the Bolivian lowlands and other proxies in Peru (Hurley et al., 2019; Kanner et al., 2013; Vuille et al., 2012). While our $\delta^{18}O_{TR}$ records also seem to capture this signal of upstream rainout, they show the highest correlations with precipitation over the Altiplano and surrounding areas (Figures 3a and 3b). This increased signal of precipitation over the Altiplano can be the result of several processes. First, a local amount effect, where more precipitation over this region results in more depleted precipitation $\delta^{18}O$ (the heavier isotopologues, $H_2{}^{18}O$, tend to collect in the precipitation, leaving the water vapor and subsequent precipitation isotopically lighter). Second, local evaporation covaries strongly with precipitation over the Altiplano (Vuille & Keimig, 2004). Cloudy and rainy conditions reduce solar radiation and temperature; hence, evaporation is reduced and soil water is less enriched in heavy isotopes. This effect may contribute to the enhanced local precipitation signal seen in our $\delta^{18}O_{TR}$ records. Third, the $\delta^{18}O_{TR}$ signature not only depends on source water $\delta^{18}O$, but can also reflect evaporative conditions at leaf level during plant transpiration, where drier conditions can result in enriched plant water $\delta^{18}O$ due to the preferential evaporation of the lighter isotope (^{16}O) (Barbour et al., 2004; Roden & Ehleringer, 1999). Under increased aridity, however, Pex (the fraction of carbonyl oxygen atoms that exchange at the cambium during biosynthesis) increases, inducing decreased $\delta^{18}O_{TR}$ (Cheesman & Cernusak, 2017; Szejner et al., 2020), which

may partly counterbalance the effect of leaf transpiration. Overall, we interpret the signal in our $\delta^{18}O_{TR}$ records to be associated with (a) upstream rainout over the Amazon basin, (b) the local precipitation amount effect, (c) an effect of local evaporation on soil water in the Altiplano, and (d) potential physiological processes at the tree level (Rodriguez-Caton et al., 2021). This would result in $\delta^{18}O_{TR}$ being a valuable proxy for hydroclimate over the Altiplano, sensitive to local precipitation, local evaporation, and upstream rainout.

The width of the rings of *P. tarapacana* is also a valuable proxy for precipitation and moisture changes in this area. However, tree-ring width records show opposite relationships with climate between consecutive growing seasons (e.g., Soliz et al., 2009) with the signal of the previous year being most useful for reconstructing precipitation (Morales et al., 2012). The climate signal of *P. tarapacana* $\delta^{18}O_{TR}$ is consistent across seasons and strongest for the current growing season (for a detailed analysis, see Rodriguez-Caton et al., 2021). Although measuring $\delta^{18}O_{TR}$ can be expensive and time consuming, $\delta^{18}O_{TR}$ provides complementary information to tree-ring width and has lower tree-to-tree variability (i.e., five trees are sufficient to capture the common variability in our *P. tarapacana* stands).

The depletion of heavy isotopes in precipitation $\delta^{18}O$ and ice-core $\delta^{18}O$ with elevation (Figure 1) is consistent with prior observations on the isotopic composition of precipitation in the Bolivian and Chilean Altiplano (Aravena et al., 1999; Fiorella et al., 2015; Hardy et al., 2003; Valdivielso et al., 2020). In contrast, $\delta^{18}O_{TR}$ seems to reflect the northeast-southwest aridity gradient across the region with more negative values for *Cedrela odorata* east of the Andes in the wetter tropical lowlands of Peru and Bolivia (Baker et al., 2015; Brienen et al., 2012) and more positive values for semiarid high-elevation *P. tarapacana* (Ballentyne et al., 2011; Rodriguez-Caton et al., 2021). Similarly, the more enriched $\delta^{18}O_{TR}$ signatures toward the southern and more arid sites of our network (Table S1 in Supporting Information S1) are likely due to reduced precipitation and therefore reduced cloudiness and higher solar radiation, driving higher soil-water evaporation and leaf transpiration.

Toward the southern portion of our study area, the $\delta^{18}O_{TR}$ variability seems to be less influenced by SST changes in the tropical Pacific, and the JFM precipitation signal is slightly weakened. The weaker strength of El Niño signal in the $\delta^{18}O_{TR}$ chronologies from the southern drier sites in comparison with the northernmost wetter sites reflects the weaker influence of El Niño in precipitation over the southwestern Altiplano (Figure S5 in Supporting Information S1) and agrees with the pattern of ENSO sensitivity reported for a network of *P. tarapanca* chronologies across the Altiplano (Crispín-DelaCruz et al., 2022). In addition, the significant negative correlation between $\delta^{18}O_{TR}$ and precipitation to the southeast of the Andes (i.e., north-central Argentina), most evident in the southern sites, suggests a possible influence of interannual variations in the intensity of the South American Low-Level Jet and extratropical cold air incursions (Garreaud, 2000; Vuille & Keimig, 2004). The southern sites (20–22°S) are located at the southern latitudinal limit of the SASM influence in the transition zone between the tropics and the subtropics, where complex interactions between atmospheric processes in low latitudes and midlatitudes may affect the $\delta^{18}O_{TR}$ precipitation signal. How these multiple factors may influence the $\delta^{18}O_{TR}$ climate signal of the southern sites deserves an in-depth analysis and will be assessed in future work. Despite the differences along the gradient, the composite $\delta^{18}O_{TR}$ chronology, explaining almost 80% of the $\delta^{18}O_{TR}$ total variability, is strongly related to both austral summer precipitation and tropical Pacific SSTs.

Stable oxygen isotopes in the tree rings of the long-lived species *P. tarapacana* hold immense promise for reconstructing tropical South American hydroclimate of the past millennium. The strong and highly consistent precipitation signal embedded along the new network of $\delta^{18}O_{TR}$ chronologies in the Altiplano represents a new tool for evaluating year-to-year and multi-centennial precipitation variability in this region. Our findings are relevant for generating more reliable regional and local hydroclimate reconstructions in the Central Andes, as well as potentially contributing to reconstruct past ENSO variability. This will be useful for improving global circulation models and providing information for a better management of water resources in this region.

Conflict of Interest

The authors declare no conflicts of interest relevant to this study.

Data Availability Statement

The tree-ring stable oxygen isotopic data for the four sites and the regional instrumental precipitation data is available at https://www.ncei.noaa.gov/access/paleo-search/study/34812noaa. IsoGSM data were retrieved from https://isotope.iis.u-tokyo.ac.jp/~kei/tmp/isogsm2/, GNIP data from https://nucleus.iaea.org/wiser/index.aspxiaea, and Ice core data from https://www.ncdc.noaa.gov/data-access/paleoclimatology-datanoaa. CRU data were downloaded from https://crudata.uea.ac.uk/cru/data/hrg/uea, CHIRPS from https://www.chc.ucsb.edu/data/chirpsucsb, ERA from https://cds.climate.copernicus.eu/cdsapp#!/dataset/reanalysis-era5-single-levels-monthly-means?tab=formcopernicus, and SSTs from https://www.ncdc.noaa.gov/data-access/marineocean-data/extended-reconstructed-sea-surface-temperature-ersst-v5#:~:text=The%20Extended%20Reconstructed%20Sea%20Surface,completeness%20enhanced%20using%20statistical%20methodsnoaa.

Acknowledgments

The authors thank Wei Wang for help with $\delta^{18}O_{TR}$ measurements and the members of the Tree-Ring Lab at Lamont-Doherty Earth Observatory for useful discussions of results. The authors are grateful to the Chilean Forest Service CONAF for permission to collect the tree-ring samples at Las Vicuñas National Reserve. This research was supported by the project THEMES funded by Foundation BNP Paribas Climate Initiative program; United States National Science Foundation (OISE-1743738, PLR-1504134, AGS-1702789, and AGS-1702439); and Lamont-Doherty Earth Observatory Climate Center. M. Rodriguez-Caton and L. Andreu-Hayles were partly funded by the Columbia University's Center for Climate and Life, and L. Andreu-Hayles also by NSF AGS-1903687. D. A. Christie was supported by Agencia Nacional de Investigación y Desarrollo (FONDECYT 1201411 and FONDAP 15110009). M. S. Morales was partly funded by Agencia Nacional de Promoción Científica y Tecnológica PICT 2013-1880; Consejo Nacional de Investigaciones Científicas y Técnicas de Argentina (PIP CONICET 11220130100584); and Proyecto Fondo Nacional de Desarrollo Científico, Tecnológico y de Innovación Tecnológica a Banco Mundial (FONDECYT-BMINC. INV 039-2019). M. P. Rao was supported by the NOAA Climate and Global Change Postdoctoral Fellowship Program, administered by UCAR's Cooperative Programs for the Advancement of Earth System Science (CPAESS) under award #NA18NWS4620043B. The authors are grateful to the anonymous reviewers for their helpful comments on an earlier version of the manuscript.

References

Aravena, R., Suzuki, O., Peña, H., Pollastri, A., Fuenzalida, H., & Grilli, A. (1999). Isotopic composition and origin of the precipitation in Northern Chile. *Applied Geochemistry*, *14*(4), 411–422. https://doi.org/10.1016/S0883-2927(98)00067-5

Argollo, J., Soliz, C., & Villalba, R. (2004). Potencialidad dendrocronológica de Polylepis tarapacana en los Andes Centrales de Bolivia. *Dendrocronological potential of Polylepis tarapacana in the Central Andes of Bolivia*, *39*(1), 5–24.

Baker, J. C. A., Gloor, M., Spracklen, D. V., Arnold, S. R., Tindall, J. C., Clerici, S. J., et al. (2016). What drives interannual variation in tree ring oxygen isotopes in the Amazon? *Geophysical Research Letters*, *43*(22), 11831–11840. https://doi.org/10.1002/2016GL071507

Baker, J. C. A., Hunt, S. F. P., Clerici, S. J., Newton, R. J., Bottrell, S. H., Leng, M. J., et al. (2015). Oxygen isotopes in tree rings show good coherence between species and sites in Bolivia. *Global and Planetary Change*, *133*, 298–308. https://doi.org/10.1016/j.gloplacha.2015.09.008

Ballantyne, A. P., Baker, P. A., Chambers, J. Q., Villalba, R., & Argollo, J. (2011). Regional differences in South American monsoon precipitation inferred from the growth and isotopic composition of tropical trees. *Earth Interactions*, *15*(5), 1–35. https://doi.org/10.1175/2010EI277.1

Barbour, M. M., Roden, J. S., Farquhar, G. D., & Ehleringer, J. R. (2004). Expressing leaf water and cellulose oxygen isotope ratios as enrichment above source water reveals evidence of a Péclet effect. *Oecologia*, *138*, 426–435. https://doi.org/10.1007/s00442-003-1449-3

Bariac, T., Jusserand, C., & Mariotti, A. (1990). Evolution spatio-temporelle de la composition isotopique de l'eau dans le continuum sol-plante-atmosphere. *Geochimica et Cosmochimica Acta*, *54*, 413–424. https://doi.org/10.1016/0016-7037(90)90330-n

Biondi, F., & Waikul, K. (2004). DENDROCLIM2002: A C++ program for statistical calibration of climate signals in tree-ring chronologies. *Computers & Geosciences*, *30*(3), 303–311. https://doi.org/10.1016/j.cageo.2003.11.004

Braun, G. (1997). The use of digital methods in assessing forest patterns in an Andean environment: The Polylepis example. *Mountain Research and Development*, *17*, 253–262. https://doi.org/10.2307/3673852

Brienen, R. J. W., Helle, G., Pons, T. L., Guyot, J.-L., & Gloor, M. (2012). Oxygen isotopes in tree rings are a good proxy for Amazon precipitation and El Niño-Southern Oscillation variability. *Proceedings of the National Academy of Sciences*, *109*(42), 16957–16962. https://doi.org/10.1073/pnas.1205977109

Canedo-Rosso, C., Hochrainer-Stigler, S., Pflug, G., Condori, B., & Berndtsson, R. (2021). Drought impact in the Bolivian Altiplano agriculture associated with the El Niño-Southern Oscillation using satellite imagery data. *Natural Hazards and Earth System Sciences*, *21*(3), 995–1010. https://doi.org/10.5194/nhess-21-995-2021

Cheesman, A. W., & Cernusak, L. A. (2017). Infidelity in the outback: Climate signal recorded in Δ18O of leaf but not branch cellulose of eucalypts across an Australian aridity gradient. *Tree Physiology*, *37*, 554–564. https://doi.org/10.1093/treephys/tpw121

Christie, D. A., Lara, A., Barichivich, J., Villalba, R., Morales, M. S., & Cuq, E. (2009). El Niño-Southern Oscillation signal in the world's highest-elevation tree-ring chronologies from the Altiplano, Central Andes. *Palaeogeography, Palaeoclimatology, Palaeoecology*, *281*, 309–319. https://doi.org/10.1016/j.palaeo.2007.11.013

Crispín-DelaCruz, D. B., Morales, M. S., Andreu-Hayles, L., Christie, D. A., Guerra, A., & Requena-Rojas, E. J. (2022). High ENSO sensitivity in tree rings from a northern population of Polylepis tarapacana in the Peruvian Andes. *Dendrochronologia*, *71*, 125902. https://doi.org/10.1016/j.dendro.2021.125902

Dawson, T. E., & Ehleringer, J. R. (1993). Isotopic enrichment of water in the "woody" tissues of plants: Implications for plant water source, water uptake, and other studies which use the stable isotopic composition of cellulose. *Geochimica et Cosmochimica Acta*, *57*, 3487–3492. https://doi.org/10.1016/0016-7037(93)90554-a

Dee, D. P., Uppala, S. M., Simmons, A. J., Berrisford, P., Poli, P., Kobayashi, S., et al. (2011). The ERA-Interim reanalysis: Configuration and performance of the data assimilation system. *Quarterly Journal of the Royal Meteorological Society*, *137*(656), 553–597. https://doi.org/10.1002/qj.828

Fiorella, R. P., Poulsen, C. J., Zolá, R. S. P., Barnes, J. B., Tabor, C. R., & Ehlers, T. A. (2015). Spatiotemporal variability of modern precipitation $\delta^{18}O$ in the central Andes and implications for paleoclimate and paleoaltimetry estimates. *Journal of Geophysical Research: Atmospheres*, *120*, 4630–4656. https://doi.org/10.1002/2014JD022893

Funk, C., Peterson, P., Landsfeld, M., Pedreros, D., Verdin, J., Shukla, S., et al. (2015). The climate hazards infrared precipitation with stations–A new environmental record for monitoring extremes. *Scientific Data*, *2*, 1–21. https://doi.org/10.1038/sdata.2015.66

Galewsky, J., & Samuels-Crow, K. (2015). Summertime moisture transport to the southern South American Altiplano: Constraints from in situ measurements of water vapor isotopic composition. *Journal of Climate*, *28*(7), 2635–2649. https://doi.org/10.1175/JCLI-D-14-00511.1

Garreaud, R., Vuille, M., & Clement, A. C. (2003). The climate of the Altiplano: Observed current conditions and mechanisms of past changes. *Palaeogeography, Palaeoclimatology, Palaeoecology*, *194*(1–3), 5–22. https://doi.org/10.1016/S0031-0182(03)00269-4

Garreaud, R. D. (1999). Multiscale analysis of the summertime precipitation over the central Andes. *Monthly Weather Review*, *127*(5), 9012–921. https://doi.org/10.1175/1520-0493(1999)127<0901:maotsp>2.0.co;2

Garreaud, R. D. (2000). Cold air incursions over subtropical South America: Mean structure and dynamics. *Monthly Weather Review*, *128*(7 II), 2544–2559. https://doi.org/10.1175/1520-0493(2000)128<2544:caioss>2.0.co;2

Gessler, A., Brandes, E., Buchmann, N., Helle, G., Rennenberg, H., & Barnard, R. L. (2009). Tracing carbon and oxygen isotope signals from newly assimilated sugars in the leaves to the tree-ring archive. *Plant, Cell and Environment*, *32*(7), 780–795. https://doi.org/10.1111/j.1365-3040.2009.01957.x

Hardy, D. R., Vuille, M., & Bradley, R. S. (2003). Variability of snow accumulation and isotopic composition on Nevado Sajama, Bolivia. *Journal of Geophysical Research*, *108*, D224693. https://doi.org/10.1029/2003JD003623

Harris, I., Osborn, T. J., Jones, P., & Lister, D. (2020). Version 4 of the CRU TS monthly high-resolution gridded multivariate climate dataset. *Scientific Data*, *7*(1), 1–18. https://doi.org/10.1038/s41597-020-0453-3

Hoffmann, G., Ramirez, E., Taupin, J. D., Francou, B., Ribstein, P., Delmas, R., et al. (2003). Coherent isotope history of Andean ice cores over the last century. *Geophysical Research Letters*, *30*(4), 1–4. https://doi.org/10.1029/2002GL014870

Hurley, J. V., Vuille, M., & Hardy, D. R. (2019). On the interpretation of the ENSO signal embedded in the stable isotopic composition of Quelccaya Ice Cap, Peru. *Journal of Geophysical Research*, *124*, 131–145. https://doi.org/10.1029/2018JD029064

Kanner, L. C., Burns, S. J., Cheng, H., Edwards, R. L., & Vuille, M. (2013). High-resolution variability of the South American summer monsoon over the last seven millennia: Insights from a speleothem record from the central Peruvian Andes. *Quaternary Science Reviews*, *75*, 1–10. https://doi.org/10.1016/j.quascirev.2013.05.008

Lenters, J. D., & Cook, K. H. (1997). On the origin of the Bolivian high and related circulation features of the South American climate. *Journal of the Atmospheric Sciences*, *54*(5), 656–678. https://doi.org/10.1175/1520-0469(1997)054<0656:otootb>2.0.co;2

Marengo, J. A., Liebmann, B., Grimm, A. M., Misra, V., Silva Dias, P. L., Cavalcanti, I. F. A., et al. (2012). Recent developments on the South American monsoon system. *International Journal of Climatology*, *32*(1), 1–21. https://doi.org/10.1002/joc.2254

Minvielle, M., & Garreaud, R. D. (2011). Projecting rainfall changes over the south American Altiplano. *Journal of Climate*, *24*(17), 4577–4583. https://doi.org/10.1175/jcli-d-11-00051.1

Morales, M. S., Christie, D. A., Villalba, R., Argollo, J., Pacajes, J., Silva, J. S., et al. (2012). Precipitation changes in the South American Altiplano since 1300 AD reconstructed by tree-rings. *Climate of the Past*, *8*(2), 653–666. https://doi.org/10.5194/cp-8-653-2012

Morales, M. S., Cook, E. R., Barichivich, J., Christie, D. A., Villalba, R., LeQuesne, C., et al. (2020). 600 years of South American tree rings reveal an increase in severe hydroclimatic events since mid-20th century. *Proceedings of the National Academy of Sciences*, *117*, 16816–16823. https://doi.org/10.1073/pnas.2002411117

Morales, M. S., Villalba, R., Grau, H. R., & Paolini, L. (2004). Rainfall-controlled tree growth in high-elevation subtropical treelines. *Ecology*, *85*(11), 3080–3089. https://doi.org/10.1890/04-0139

Moya, J., & Lara, A. (2011). Tree rings chronologies of quenoa (Polylepis tarapacana) for the last 500 years in the Altiplano of Arica and parinacota region, Chile. *Bosque*, *32*(2), 165–173. https://doi.org/10.4067/S0717-92002011000200007

Neukom, R., Rohrer, M., Calanca, P., Salzmann, N., Huggel, C., Acuna, D., et al. (2015). Facing unprecedented drying of the Central Andes? Precipitation variability over the period 1000–2100. *Environmental Research Letters*, *10*, 084017. https://doi.org/10.1088/1748-9326/10/8/084017

R Core Team. (2020). *R: A language and environment for statistical computing*. R Foundation for Statistical Computing. Retrieved from https://www.R-project.org/

Raia, A., & Cavalcanti, I. F. A. (2008). The life cycle of the South American monsoon system. *Journal of Climate*, *21*(23), 6227–6246. https://doi.org/10.1175/2008JCLI2249.1

Rathgeber, C. B. K., Cuny, H. E., & Fonti, P. (2016). Biological basis of tree-ring formation: A crash course. *Frontiers of Plant Science*, *7*(MAY2016), 1–7. https://doi.org/10.3389/fpls.2016.00734

Risi, C., Bony, S., & Vimeux, F. (2012). Influence of convective processes on the isotopic composition ($\delta^{18}O$ and δD) of precipitation and water vapor in the Tropics, Part 2: Physical interpretation of the amount effect. *Journal of Geophysical Research*, *113*, D19306. https://doi.org/10.1029/2008JD009943

Roden, J. S., & Ehleringer, A. R. (1999). Observations of hydrogen and oxygen isotopes in leaf water confirm the Craig-Gordon model under wide-ranging environmental conditions. *Plant Physiology*, *120*, 1165–1174. https://doi.org/10.1104/pp.120.4.1165

Rodriguez-Caton, M., Andreu-Hayles, L., Morales, M. S., Daux, V., Christie, D. A., Coopman, R. E., et al. (2021). Different climate sensitivity for radial growth, but uniform for tree-ring stable isotopes along an aridity gradient in Polylepis tarapacana, the world's highest elevation tree species. *Tree Physiology*, *41*(8), 1353–1371. https://doi.org/10.1093/treephys/tpab021

Segura, H., Espinoza, J. C., Junquas, C., Lebel, T., Vuille, M., & Garreaud, R. (2020). Recent changes in the precipitation-driving processes over the southern tropical Andes/western Amazon. *Climate Dynamics*, *54*, 2613–2631. https://doi.org/10.1007/s00382-020-05132-6

Smith, T. M., Reynolds, R. W., Peterson, T. C., & Lawrimore, J. (2008). Improvements to NOAA's historical merged land-ocean surface temperature analysis (1880-2006). *Journal of Climate*, *21*. https://doi.org/10.1175/2007jcli2100.1

Solíz, C., Villalba, R., Argollo, J., Morales, M. S., Christie, D. A., Moya, J., & Pacajes, J. (2009). Spatio-temporal variations in Polylepis tarapacana radial growth across the Bolivian Altiplano during the 20th century. *Palaeogeography, Palaeoclimatology, Palaeoecology*, *281*(3–4), 296–308. https://doi.org/10.1016/j.palaeo.2008.07.025

Sternberg, L. D. S. L., Deniro, M. J., & Savidge, R. A. (1986). Oxygen isotope exchange between metabolites and water during biochemical reactions leading to cellulose synthesis. *Plant Physiology*, *82*(2), 423–427. https://doi.org/10.1104/pp.82.2.423

Sulca, J., Takahashi, K., Espinoza, J.-C., Vuille, M., & Lavado, W. (2018). Impacts of different ENSO flavors and tropical Pacific convection variability (ITCZ, SPCZ) on austral summer rainfall in South America, with a focus on Peru. *International Journal of Climatology*, *38*, 420–435. https://doi.org/10.1002/joc.5185

Szejner, P., Clute, T., Anderson, E., Evans, M. N., & Hu, J. (2020). Reduction in lumen area is associated with the δ 18 O exchange between sugars and source water during cellulose synthesis. *New Phytologist*, *226*, 1583–1593. https://doi.org/10.1111/nph.16484

Thompson, L. G., Davis, M. E., Mosley-Thompson, E., Sowers, T. A., Henderson, K. A., Zagorodnov, V. S., et al. (1998). A 25,000-year tropical climate history from Bolivian ice cores. *Science*, *282*(5395), 1858–1864. https://doi.org/10.1126/science.282.5395.1858

Thompson, L. G., Mosley-Thompson, E., & Arnao, B. M. (1984). El Niño-Southern Oscillation events recorded in the stratigraphy of the tropical Quelccaya ice cap, Peru. *Science*, *226*(4670), 50–53. https://doi.org/10.1126/science.226.4670.50

Valdivielso, S., Vázquez-Suñé, E., & Custodio, E. (2020). Origin and variability of oxygen and hydrogen isotopic composition of precipitation in the Central Andes: A review. *Journal of Hydrology*, *587*(December 2019), 124899. https://doi.org/10.1016/j.jhydrol.2020.124899

Vautard, R. (1995). Patterns in time: SSA and MSSA. In H. von Storch, & A. Navarra (Eds.), *Analysis of climate variability. Applications of statistical techniques* (pp. 259–279). Springer. https://doi.org/10.1007/978-3-662-03167-4_14

Vautard, R., & Ghil, M. (1989). Singular spectrum analysis in nonlinear dynamics, with applications to paleoclimatic time series. *Physica D: Nonlinear Phenomena*, *35*, 395–424. https://doi.org/10.1016/0167-2789(89)90077-8

Vimeux, F., Gallaire, R., Bony, S., Hoffmann, G., & Chiang, J. C. H. (2005). What are the climate controls on δD in precipitation in the Zongo Valley (Bolivia)? Implications for the Illimani ice core interpretation. *Earth and Planetary Science Letters*, *240*(2), 205–220. https://doi.org/10.1016/j.epsl.2005.09.031

Vimeux, F., Ginot, P., Schwikowski, M., Vuille, M., Hoffmann, G., Thompson, L. G., & Schotterer, U. (2009). Climate variability during the last 1000 years inferred from Andean ice cores: A review of methodology and recent results. *Palaeogeography, Palaeoclimatology, Palaeoecology*, *281*(3–4), 229–241. https://doi.org/10.1016/j.palaeo.2008.03.054

Vimeux, F., Tremoy, G., Risi, C., & Gallaire, R. (2011). A strong control of the South American SeeSaw on the intra-seasonal variability of the isotopic composition of precipitation in the Bolivian Andes. *Earth and Planetary Science Letters*, *307*, 47–58. https://doi.org/10.1016/j.epsl.2011.04.031

Vuille, M. (1999). Atmospheric circulation over the Bolivian Altiplano during dry and wet periods and extreme phases of the southern oscillation. *International Journal of Climatology*, *19*(14), 1579–1600. https://doi.org/10.1002/(sici)1097-0088(19991130)19:14<1579::aid-joc441>3.0.co;2-n.-N

Vuille, M., & Ammann, C. (1997). Regional snowfall patterns in the high arid Andes. *Climatic Change*, *36*, 413–423. https://doi.org/10.1023/a:1005330802974

Vuille, M., Burns, S. J., Taylor, B. L., Cruz, F. W., Bird, B. W., Abbott, M. B., et al. (2012). A review of the South American monsoon history as recorded in stable isotopic proxies over the past two millennia. *Climate of the Past*, *8*, 1309–1321. https://doi.org/10.5194/cp-8-1309-2012

Vuille, M., & Keimig, F. (2004). Interannual variability of summertime convective cloudiness and precipitation in the central Andes derived from ISCCP-B3 data. *Journal of Climate*, *17*(17), 33342–3348. https://doi.org/10.1175/1520-0442(2004)017<3334:ivoscc>2.0.co;2

Vuille, M., & Werner, M. (2005). Stable isotopes in precipitation recording South American summer monsoon and ENSO variability: Observations and model results. *Climate Dynamics*, *25*(4), 401–413. https://doi.org/10.1007/s00382-005-0049-9

Yoshimura, K., Kanamitsu, M., Noone, D., & Oki, T. (2008). Historical isotope simulation using Reanalysis atmospheric data. *Journal of Geophysical Research*, *113*(19), 1–15. https://doi.org/10.1029/2008JD010074

Zang, C., & Biondi, F. (2015). treeclim: An R package for the numerical calibration of proxy-climate relationships. *Ecography*, *38*(4), 431–436. https://doi.org/10.1111/ecog.01335